CARPATHIAN J. MATH.
Volume **42** ( ), No. 1,
Pages 1-11

Online version at https://www.carpathian.cunbm.utcluj.ro/
Print Edition: ISSN 1584 - 2851; Online Edition: ISSN 1843 - 4401
DOI: https://doi.org/

Numerical Approximation for an Axisymmetric Brinkman Exterior Problem

KHALED M'HAMED-MESSAOUD[1], RABAH HACENE BELLOUT[2], AND TOUFIK LAADJ[3]

ABSTRACT. This paper presents a novel numerical approximation of the axisymmetric Brinkman flow in three-dimensional exterior domains using the infinite element method, offering a robust alternative to conventional boundary element methods. By extending the framework established for the axisymmetric Stokes problem, we develop a stable and convergent approach for the Brinkman equations, accommodating a wide range of inverse permeability parameter. Numerical experiments for both Stokes and Brinkman problems demonstrate first-order convergence under the $\mathbf{L}_1^2$ norm, with the method maintaining stability across various parameter settings and large unbounded domains. Our results highlight the efficacy and versatility of the infinite element method, making it a promising tool for solving complex fluid flow problems in exterior domains.

1. INTRODUCTION

The Brinkman equations model the flow of a viscous fluid through porous media, serving as a parameter-dependent bridge between the Darcy and Stokes models. Initially introduced as a homogenization technique for the Navier-Stokes equations [1], the Brinkman model finds applications in diverse fields such as underground water hydrology, petroleum engineering, automotive industry, biomedical engineering, and heat pipe modeling. Its unified formulation offers a significant advantage over domain decomposition methods that couple Darcy and Stokes equations, particularly in scenarios where the number and locations of Stokes-Darcy interfaces are unknown a priori.

Despite its versatility, solving the Brinkman equations poses significant challenges, especially due to the high variability in the partial differential equation (PDE) coefficients, which can take extremely large or small values. This variability adversely affects the conditioning of the discrete problem, complicating the development of stable finite element discretizations [25, 23]. Various finite element families have been tested for Brinkman flow, with studies such as [16, 21] demonstrating that optimal convergence in the Darcy case is achieved using $P_k - P_{k-1}$ polynomials for pressure and velocity, respectively, while the reverse holds for the Stokes case. To address this, equal-order interpolation has been recommended for robust performance across all parameter regimes.

Efforts to enhance numerical stability include the work of Burman and Hansbo [7, 8], who introduced jump penalization on velocity or pressure fields to stabilize Crouzeix-Raviart or $P_1 - P_0$ elements. Similarly, Correa and Loula [9] employed an augmented Lagrangian approach with least-squares stabilization to extend the applicability of Taylor-Hood elements to the Darcy case. High-order non-conforming elements were explored by Guzmán and Neilan [15], while Vassilevski and Villa [24] highlighted limitations of certain finite element pairs in extreme parameter regimes, such as the Darcy limit where viscosity $\sigma \to 0$ or impermeability $\varkappa \to \infty$.

Received: 03.04.2025. In revised form: 22.08.2025. Accepted: 10.09.2025
2020 *Mathematics Subject Classification.* 65Mxx, 76D07, 76D99.
Key words and phrases. *Brinkman problem, exterior problems, infinite element method, numerical approximation.*
Corresponding author: Toufik Laadj; toufik.laadj@usthb.edu.dz

For exterior domains, boundary integral methods have been widely used, as seen in the work of Kohr and Wendland [18], who addressed a transmission problem for Brinkman flow around a porous particle using Fredholm integral equations. Recent studies by Kohr et al. [19, 20], Gutt et al. [14], and Anaya et al. [2] have further advanced the understanding of Brinkman flow through vorticity formulations and other approaches.

This study introduces a novel application of the infinite element method, inspired by Ying [27, 28], to the numerical approximation of the axisymmetric Brinkman problem in three-dimensional exterior domains. Unlike the commonly used boundary element methods [6, 22, 17], our approach leverages the infinite element method to handle unbounded domains effectively. Building on the well-posedness results for the axisymmetric Stokes problem [4, 12, 13, 5, 3], we extend the framework of Fang and Liao [11] to the Brinkman problem. Our contribution lies in demonstrating the stability and convergence of the infinite element method for a wide range of inverse permeability parameters $\varkappa$, validated through numerical experiments for both Stokes and Brinkman problems. These experiments confirm the method's robustness in large unbounded domains, offering a computationally efficient alternative to traditional approaches.

Recent advancements in numerical methods for the Brinkman problem include the virtual element method (VEM), which accommodates general polygonal meshes. For instance, Xiong and Chen [26] developed a pressure-robust VEM with a priori and a posteriori error estimates, achieving viscosity-independent convergence for the incompressible Brinkman problem. In contrast, our work employs the infinite element method to address the challenges of axisymmetric exterior domains, offering computational efficiency for unbounded regions.

The paper is structured as follows: Section 2 outlines notations and preliminaries. Section 3 formulates the axisymmetric Brinkman problem and establishes its well-posedness. Section 4 describes the infinite element approximation, while Section 5 details the implementation algorithm. Numerical results are presented in Section 6, followed by conclusions in Section 7, where we summarize the scope and main merits of this work.

2. Notations and Preliminaries

In this paper, Ω^c denotes a bounded, simply connected three-dimensional domain with Lipschitz continuous boundary $\partial\Omega^c$, where $\mathbf{n}$ is the unit outward normal. The domain Ω represents the exterior of $\overline{\Omega^c}$. Similarly, Ξ^c is an open, simply connected domain in $\mathbb{R}^2$ with boundary $\partial\Xi^c$ and unit outward normal $\widetilde{\mathbf{n}}$, and Ξ is the exterior of $\overline{\Xi^c}$. The domain Ξ serves as the meridional section of the axisymmetric domain Ω, enabling the transformation of three-dimensional axisymmetric problems into equivalent two-dimensional problems on Ξ [5].

We denote by $C^\infty(\Omega)$ the space of infinitely differentiable functions on Ω, and $C_0^\infty(\Omega)$ the subspace of functions with compact support. The space $C(\Omega)$ consists of continuous functions on Ω, and $D'(\Omega)$ is the space of distributions. For an integer $l \geq 0$ and real number p with $1 \leq p \leq \infty$, $L^p(\Omega)$ comprises measurable functions u such that $\left(\int_\Omega |u|^p \, dx\right)^{1/p} < \infty$. The Sobolev space $W^{l,p}(\Omega)$ includes functions with distributional derivatives up to order l in $L^p(\Omega)$, equipped with the norm

$$\|u\|_{l,p,\Omega} = \left(\sum_{|\alpha| \leq l} \|D^\alpha u\|_p^p \right)^{1/p}, \quad \text{or } |u|_{l,p,\Omega} = \left(\sum_{|\alpha| = l} \|D^\alpha u\|_p^p \right)^{1/p},$$

with modifications for $p = \infty$. When $p = 2$, we denote $W^{l,2}(\Omega) = H^l(\Omega)$. The space $W_0^{l,p}(\Omega)$ is the closure of $C_0^\infty(\Omega)$ under the norm $\|\cdot\|_{l,p,\Omega}$, and $(W^{l,p}(\Omega))'$ is its dual.

For axisymmetric problems, weighted Sobolev spaces are essential to account for the radial dependence and ensure well-posedness [5]. The space $H^{1,*}(\Omega)$ is defined as

$$H^{1,*}(\Omega) = \left\{ u \in D'(\Omega) : \nabla u \in \mathbf{L}^2(\Omega), \frac{u}{|\mathbf{x}|^2} \in L^2(\Omega) \right\},$$

with the norm

$$\|u\|_{1,*} = \left(\int_\Omega \left(|\nabla u|^2 + \frac{u^2}{|\mathbf{x}|^2} \right) dx \right)^{1/2}.$$

This space is the closure of $C^\infty(\Omega)$ under $\|\cdot\|_{1,*}$, and $H_0^{1,*}(\Omega)$ is the closure of $C_0^\infty(\Omega)$.

On the meridional domain Ξ, we define the weighted space $L^p_\alpha(\Xi)$ as the set of measurable functions $\widetilde{\omega}(r,z)$ satisfying

$$\|\widetilde{\omega}\|_{L^p_\alpha(\Xi)} = \left(\int_\Xi |\widetilde{\omega}|^p r^\alpha \, dr\, dz \right)^{1/p} < \infty,$$

for any real number α and $1 \le p < \infty$. The weighted Sobolev space $W_1^{l,p}(\Xi)$ consists of functions in $L_1^p(\Xi)$ whose partial derivatives up to order l belong to $L_1^p(\Xi)$, with the semi-norm and norm

$$|\widetilde{\omega}|_{W_1^{l,p}(\Xi)} = \left(\sum_{k=0}^{l} \|\partial_r^k \partial_z^{l-k} \widetilde{\omega}\|^p_{L_1^p(\Xi)} \right)^{1/p}, \quad \|\widetilde{\omega}\|_{W_1^{l,p}(\Xi)} = \left(\sum_{k=0}^{l} |\widetilde{\omega}|^p_{W_1^{k,p}(\Xi)} \right)^{1/p}.$$

When $p = 2$, we denote $W_1^{l,2}(\Xi) = H_1^l(\Xi)$. The space $H_1^s(\partial\Xi)$, for $s \ge 0$, is built from $L_1^2(\partial\Xi)$, defined as

$$L_1^2(\partial\Xi) = \left\{ g : \partial\Xi \to \mathbb{R} \text{ measurable} : \int_{\partial\Xi} g^2 r(t)\, dt < \infty \right\},$$

where $r(t)$ is the radial coordinate at the point with tangential coordinate t. The trace operator is continuous from $H_1^1(\Xi)$ to $H_1^{1/2}(\partial\Xi)$ [5].

Further, we define

$$H^1_{1,0}(\Xi) = \left\{ \widetilde{\omega} \in H_1^1(\Xi) : \widetilde{\omega}|_{\partial\Xi} = 0 \right\}, \quad V_1^1(\Xi) = \left\{ \widetilde{\omega} \in H_1^1(\Xi) : \widetilde{\omega} \in L^2_{-1}(\Xi) \right\},$$

$$V^1_{1,0}(\Xi) = \left\{ \widetilde{\omega} \in H^1_{1,0}(\Xi) : \widetilde{\omega} \in L^2_{-1}(\Xi) \right\},$$

with the norm

$$\|\widetilde{\omega}\|_{V_1^1(\Xi)} = \left(|\widetilde{\omega}|^2_{H_1^1(\Xi)} + \|\widetilde{\omega}\|^2_{L^2_{-1}(\Xi)} \right)^{1/2}.$$

The space $\mathbf{X}(\Xi) = V^1_{1,0}(\Xi) \times H^1_{1,0}(\Xi)$ is equipped with the norm

$$\|\widetilde{\mathbf{u}}\|_{\mathbf{X}} = \left(\|\widetilde{u}_1\|^2_{V_1^1(\Xi)} + |\widetilde{u}_2|^2_{H_1^1(\Xi)} \right)^{1/2}.$$

The differential operators on Ξ are defined as

$$\widetilde{\nabla}\widetilde{u} = \left(\frac{\partial \widetilde{u}}{\partial r}, \frac{\partial \widetilde{u}}{\partial z} \right), \quad \widetilde{\nabla} \cdot \widetilde{\mathbf{u}} = \frac{\partial \widetilde{u}_1}{\partial r} + \frac{\widetilde{u}_1}{r} + \frac{\partial \widetilde{u}_2}{\partial z},$$

$$\widetilde{\nabla} \times \widetilde{\mathbf{u}} = \frac{\partial \widetilde{u}_1}{\partial z} - \frac{\partial \widetilde{u}_2}{\partial r}, \quad \widetilde{\Delta}\widetilde{\mathbf{u}} = \left(-\frac{1}{r}\widetilde{\nabla}(r\widetilde{\nabla}\widetilde{u}_1) + \frac{1}{r^2}\widetilde{u}_1, -\frac{1}{r}\widetilde{\nabla}(r\widetilde{\nabla}\widetilde{u}_2) \right).$$

These definitions facilitate the transformation of axisymmetric problems into the meridional plane, ensuring proper handling of singularities near the axis of symmetry [5].

3. Axisymmetric Brinkman Exterior Problem

We consider the Brinkman problem in the exterior domain Ω:

$$-\sigma\Delta\mathbf{u} + \varkappa\mathbf{u} + \nabla p = \mathbf{f}, \qquad \text{in } \Omega, \tag{3.1}$$

$$\operatorname{div}\mathbf{u} = 0, \qquad \text{in } \Omega, \tag{3.2}$$

$$\mathbf{u}|_{\partial\Omega} = \mathbf{g}, \tag{3.3}$$

with the compatibility condition

$$\int_{\partial\Omega} \mathbf{g}\cdot\mathbf{n}\, ds = 0, \tag{3.4}$$

where $\sigma \geq 0$ is the fluid viscosity and $\varkappa$ is the inverse permeability of the porous medium. When $\varkappa$ is small, the equations approximate the Stokes problem, while large $\varkappa$ values resemble the Darcy equations [24].

The axisymmetric formulation reduces the three-dimensional problem to the meridional domain Ξ, following the framework established for the Stokes problem [5, 11]. As shown in [5], the axisymmetric Stokes system splits into two problems: one for the angular component u_θ and another for (u_r, u_z, p). Assuming no rotation (i.e., $\mathbf{f}_\theta = 0$, $\mathbf{g}_\theta = 0$), the angular component $u_\theta = 0$, so $\mathbf{u} = (u_r(r,\theta,z), 0, u_z(r,\theta,z)) \leftrightarrow \widetilde{\mathbf{u}} = (\widetilde{u}_1(r,z), \widetilde{u}_2(r,z))$ and $p(r,\theta,z) \leftrightarrow \widetilde{p}(r,z)$. The same is the case for the Brinkman problem [5, 11], which we extend here by incorporating the permeability term $\varkappa\mathbf{u}$.

The stationary axisymmetric Brinkman equations with zero angular components and incompressibility are:

$$-\frac{1}{r}\widetilde{\nabla}(r\widetilde{\nabla}\widetilde{u}_1) + \frac{1}{r^2}\widetilde{u}_1 + \varkappa\widetilde{u}_1 + \frac{\partial\widetilde{p}}{\partial r} = \widetilde{f}_1, \qquad \text{in } \Xi, \tag{3.5}$$

$$-\frac{1}{r}\widetilde{\nabla}(r\widetilde{\nabla}\widetilde{u}_2) + \varkappa\widetilde{u}_2 + \frac{\partial\widetilde{p}}{\partial z} = \widetilde{f}_2, \qquad \text{in } \Xi, \tag{3.6}$$

$$\frac{\partial}{\partial r}(r\widetilde{u}_1) + \frac{\partial}{\partial z}(r\widetilde{u}_2) = 0, \qquad \text{in } \Xi, \tag{3.7}$$

$$(\widetilde{u}_1, \widetilde{u}_2)|_{\partial\Xi} = \widetilde{\mathbf{g}}, \tag{3.8}$$

with

$$\int_{\partial\Xi} r\widetilde{\mathbf{g}}\cdot\widetilde{\mathbf{n}}\, ds = 0. \tag{3.9}$$

For $\widetilde{\mathbf{g}} \in \mathbf{V}_1^{1/2}(\partial\Xi) = \left\{\widetilde{\omega} \in H_1^{1/2}(\partial\Xi) : \widetilde{\omega} \in L^2_{-1}(\partial\Xi)\right\}$ satisfying (3.9), there exists $\widetilde{\mathbf{u}}_0 \in \mathbf{V}_1^1(\Xi)$ such that $\widetilde{\nabla}\cdot\widetilde{\mathbf{u}}_0 = 0$ and $\widetilde{\mathbf{u}}_0|_{\partial\Xi} = \widetilde{\mathbf{g}}$ [5]. Setting $\overline{\mathbf{u}} = \widetilde{\mathbf{u}} - \widetilde{\mathbf{u}}_0$, the problem reduces to a homogeneous boundary system with right-hand side $\widetilde{\mathbf{f}} + \widetilde{\Delta}\widetilde{\mathbf{u}}_0$. Thus, we focus on (3.5)–(3.8) with $\widetilde{\mathbf{g}}|_{\partial\Xi} = 0$.

The variational formulation is: Given $\widetilde{\mathbf{f}} \in (\mathbf{X}(\Xi))'$, find $\widetilde{\mathbf{u}} \in \mathbf{X}(\Xi)$, $\widetilde{p} \in L^2_1(\Xi)$, such that

$$\widetilde{a}(\widetilde{\mathbf{u}}, \widetilde{\mathbf{v}}) + \widetilde{b}(\widetilde{\mathbf{v}}, \widetilde{p}) = \langle\widetilde{\mathbf{f}}, \widetilde{\mathbf{v}}\rangle_0, \qquad \forall\widetilde{\mathbf{v}} \in \mathbf{X}(\Xi), \tag{3.10}$$

$$\widetilde{b}(\widetilde{\mathbf{u}}, \widetilde{q}) = 0, \qquad \forall\widetilde{q} \in L^2_1(\Xi), \tag{3.11}$$

where $\langle\widetilde{\mathbf{f}}, \widetilde{\mathbf{v}}\rangle_0 := \int_\Xi r\widetilde{\mathbf{f}}\cdot\widetilde{\mathbf{v}}\, dr\, dz$, and the bilinear forms are

$$\widetilde{a}(\widetilde{\mathbf{u}}, \widetilde{\mathbf{v}}) = \int_\Xi \left[r\left(\widetilde{\nabla}\widetilde{u}_1\cdot\widetilde{\nabla}\widetilde{v}_1 + \widetilde{\nabla}\widetilde{u}_2\cdot\widetilde{\nabla}\widetilde{v}_2 + \frac{1}{r^2}\widetilde{u}_1\widetilde{v}_1\right) + \varkappa\left(\widetilde{u}_1\widetilde{v}_1 + \widetilde{u}_2\widetilde{v}_2\right)\right] dr\, dz, \tag{3.12}$$

$$\widetilde{b}(\widetilde{\mathbf{u}}, \widetilde{p}) = \int_\Xi \widetilde{p}\left(\frac{\partial}{\partial r}(r\widetilde{u}_1) + \frac{\partial}{\partial z}(r\widetilde{u}_2)\right) dr\, dz. \tag{3.13}$$

The well-posedness of the Stokes problem was established by Fang and Liao [11], who proved the ellipticity of $\widetilde{a}(\cdot,\cdot)$ and the inf-sup condition for $\widetilde{b}(\cdot,\cdot)$. Our contribution extends this to the Brinkman problem, where the bilinear form $\widetilde{a}(\cdot,\cdot)$ in (3.12) is elliptic since

$$\widetilde{a}(\widetilde{\mathbf{u}},\widetilde{\mathbf{u}}) = \|\widetilde{\mathbf{u}}\|^2_{\mathbf{X}(\Xi)} + \varkappa\|\widetilde{\mathbf{u}}\|^2_{L^2(\Xi)} \geq \alpha\|\widetilde{\mathbf{u}}\|^2_{\mathbf{X}(\Xi)}, \quad \alpha > 0,$$

for $\varkappa \geq 0$. The inf-sup condition

$$\inf_{\widetilde{p}\in L^2_1(\Xi)} \sup_{\widetilde{\mathbf{u}}\in\mathbf{X}(\Xi)} \frac{\widetilde{b}(\widetilde{\mathbf{u}},\widetilde{p})}{\|\widetilde{\mathbf{u}}\|_{\mathbf{X}(\Xi)}\|\widetilde{p}\|_{L^2_1(\Xi)}} \geq \beta, \quad \beta > 0, \tag{3.14}$$

holds as in the Stokes case [11]. This ensures the well-posedness of the Brinkman problem, a novel result in the context of axisymmetric exterior domains.

4. Infinite Element Approximation

We employ the infinite element method (IEM) developed by Ying [27, 28] to solve the variational system (3.10)–(3.11), adapting it to the axisymmetric Brinkman problem in exterior domains. The choice of $P_2 - P_0$ elements, where the velocity $\widetilde{\mathbf{u}}_h$ is piecewise quadratic (P_2) and the pressure $\widetilde{p}_h$ is piecewise constant (P_0), ensures stability for Stokes-like problems while accommodating the additional permeability term in the Brinkman equations [10]. This is a novel application of IEM, extending its use from the Stokes problem [11] to the more complex Brinkman model.

The triangulation $\mathcal{T}_h$ is constructed on Ξ, assuming the section boundary $\partial\Xi$ is a polygon with the origin $\mathbf{o} \in \Gamma_0 = \partial\Xi$. For a constant $\xi > 1$, similar curves $\Gamma_1, \Gamma_2, \ldots, \Gamma_k, \ldots$ are drawn with proportionality constants $\xi, \xi^2, \ldots, \xi^k$, respectively, centered at $\mathbf{o}$. The domain between Γ_{k-1} and Γ_k forms a layer Ξ_k, divided into triangles with consistent element counts across layers. Nodes on Γ_0 are selected, including all vertices, and rays from the origin divide each layer into similar quadrilaterals, each split into two triangles (see Figure 1).

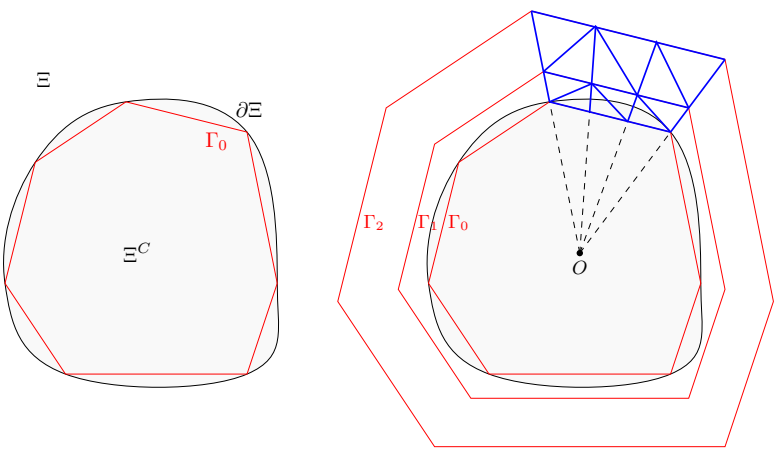

Figure 1. Infinite Element triangulation of the domain Ξ.

We require the triangulation to be of C^0 type [13] and regular, satisfying

$$\forall e \in \mathcal{T}_h, \quad \exists\sigma > 0 \text{ s.t. } \frac{h_e}{\rho_e} \leq \sigma,$$

where h_e is the longest edge of element e, and ρ_e is the diameter of the largest ball contained in e. This ensures

$$\text{meas}(e) \leq C_0 h^2 \,\text{dist}(\mathbf{o}, e)^2,$$

with C_0 a positive constant, $h = \max h_e$ in Ξ_1, and $\mathrm{dist}(\mathbf{o}, e)$ the distance from e to the origin [4].

The infinite element spaces are defined as:

$$\mathbf{S}_h = \left\{\widetilde{\mathbf{u}} \in C(\Xi)^2 : \widetilde{\mathbf{u}}|_e \in \mathbf{P}_2(e), \forall e \in \mathcal{T}_h\right\},$$

$$\mathbf{X}_h = \left\{\widetilde{\mathbf{u}} \in \mathbf{X}(\Xi) : \widetilde{\mathbf{u}} \in \mathbf{S}_h\right\}, \quad Q_h = \left\{\widetilde{p} \in L_1^2(\Xi) : \widetilde{p}|_e \in \mathbf{P}_0(e), \forall e \in \mathcal{T}_h\right\},$$

$$\mathbf{W}_h = \left\{\widetilde{\mathbf{u}} \in C(\Xi)^2 : \widetilde{\mathbf{u}} \in \mathbf{X}(\Xi), \widetilde{\mathbf{u}}|_e \in \mathbf{P}_1(e)^2, \forall e \in \mathcal{T}_h\right\}.$$

The discrete problem is: Find $(\widetilde{\mathbf{u}}_h, \widetilde{p}_h) \in \mathbf{X}_h \times Q_h$ such that

$$\widetilde{a}(\widetilde{\mathbf{u}}_h, \widetilde{\mathbf{v}}_h) + \widetilde{b}(\widetilde{\mathbf{v}}_h, \widetilde{p}_h) = \langle \widetilde{\mathbf{f}}, \widetilde{\mathbf{v}}_h \rangle_{(0)}, \qquad \forall \widetilde{\mathbf{v}}_h \in \mathbf{X}_h, \tag{4.15}$$

$$\widetilde{b}(\widetilde{\mathbf{u}}_h, \widetilde{q}_h) = 0, \qquad \forall \widetilde{q}_h \in Q_h. \tag{4.16}$$

The well-posedness of this saddle point problem follows from the Babuŝka-Brezzi-Neĉas theorem [10]. The bilinear form $\widetilde{a}(\cdot,\cdot)$ is coercive, and the inf-sup condition is verified as in [11], ensuring convergence as $h \to 0$.

5. Implementation

The infinite element method (IEM) proposed by Ying [27, 28] offers a computationally efficient approach for solving the Brinkman equations in unbounded domains by avoiding domain truncation, unlike boundary element methods. We implement the algorithm for the homogeneous case ($\widetilde{\mathbf{f}} = 0$), following [27, 28], with extensions to the non-homogeneous case possible as described therein.

The values of $\widetilde{\mathbf{u}}_h$ at the nodes on the polygon Γ_k are arranged into the column vector

$$\mathbf{y}_k = \left(\widetilde{v}_h^{(1)}, \widetilde{u}_h^{(2)}, \widetilde{v}_h^{(2)}, \widetilde{u}_h^{(3)}, \widetilde{v}_h^{(3)}, \ldots, \widetilde{u}_h^{(N-1)}, \widetilde{v}_h^{(N-1)}, \widetilde{v}_h^{(N)}\right)^t,$$

where $\widetilde{u}_h^{(j)}$ and $\widetilde{v}_h^{(j)}$ denote the r- and z-direction components of $\widetilde{\mathbf{u}}_h$ at the j-th node, respectively, and N is the number of nodes on each Γ_k. Due to the symmetry of the domain, the r-component of $\widetilde{\mathbf{u}}_h$ is zero on the axis of symmetry.

Since the boundary value $\widetilde{\mathbf{g}}_h$ must satisfy the compatibility condition $\int_{\Gamma_0} r\widetilde{\mathbf{g}}_h \cdot \widetilde{\mathbf{n}}\, ds = 0$, there exists a vector $\mathbf{h}$ such that $\mathbf{h}^T\mathbf{y}_0 = 0$. To enforce this condition on all layers without imposing it directly, we select a test function $\widetilde{q}$ in equation (3.11) such that $\widetilde{q} = 0$ on $\xi^k\Xi$ and $\widetilde{q} = 1$ on $\Xi \setminus \xi^k\Xi$. This yields

$$0 = \int_{\Xi\setminus\xi^k\Xi} r\widetilde{\nabla} \cdot \widetilde{\mathbf{u}}\, dr\, dz = \int_{\Gamma_0} r\widetilde{\mathbf{u}} \cdot \widetilde{\mathbf{n}}\, ds + \int_{\Gamma_k} r\widetilde{\mathbf{u}} \cdot \widetilde{\mathbf{n}}\, ds.$$

Given the compatibility condition on Γ_0, it follows that $\int_{\Gamma_k} r\widetilde{\mathbf{u}} \cdot \widetilde{\mathbf{n}}\, ds = 0$, or equivalently, $\mathbf{h}^T\mathbf{y}_k = 0$ for all k.

We normalize $\mathbf{h}$ to a unit vector and construct an orthogonal matrix $T = [\mathbf{h}, H]$, where $\mathbf{h}$ is the first column. Setting $\mathbf{z}_k = H^T\mathbf{y}_k$ establishes a one-to-one correspondence between $\mathbf{z}_k$ and $\mathbf{y}_k$, effectively incorporating the flux condition.

We solve the Brinkman equations on Ξ_1 using the finite element method with boundary data $\mathbf{y}_0$ and $\mathbf{y}_1$ on the given mesh, after eliminating the degrees of freedom associated with mid-edge points $\mathbf{y}_{1/2}$ via static condensation. Let the approximate solution be $\widetilde{\mathbf{u}}_h$. Then, there exist matrices K_0, K_0', and A such that

$$\widetilde{a}(\widetilde{\mathbf{u}}_h, \widetilde{\mathbf{v}}_h) = (\mathbf{z}_0^T, \mathbf{z}_1^T) \begin{pmatrix} K_0 & -A^T \\ -A & K_0' \end{pmatrix} \begin{pmatrix} \mathbf{z}_0 \\ \mathbf{z}_1 \end{pmatrix}, \tag{5.17}$$

where the block matrix is the stiffness matrix for the layer between Γ_0 and Γ_1.

Owing to the geometric similarity of the layers Ξ_k, the stiffness matrices for subsequent layers are scaled by factors of ξ^{k-1}, yielding

$$\xi^{k-1}\begin{pmatrix} K_0 & -A^T \\ -A & K_0' \end{pmatrix}, \quad k = 2, 3, \ldots.$$

Assembling these layer stiffness matrices at the nodes results in the infinite system of equations:

$$\begin{aligned} -A\mathbf{z}_0 + \xi^{1/2}K\mathbf{z}_1 - \xi A^T\mathbf{z}_2 &= 0, \\ -A\mathbf{z}_1 + \xi^{1/2}K\mathbf{z}_2 - \xi A^T\mathbf{z}_3 &= 0, \\ &\vdots \\ -A\mathbf{z}_{k-1} + \xi^{1/2}K\mathbf{z}_k - \xi A^T\mathbf{z}_{k+1} &= 0, \\ &\vdots \end{aligned} \tag{5.18}$$

where $K = \xi^{1/2}K_0 + \xi^{-1/2}K_0'$.

As shown by Ying in [27, 28], there exists a real transfer matrix X such that

$$\mathbf{z}_{k+1} = X\mathbf{z}_k, \quad k = 0, 1, \ldots. \tag{5.19}$$

Starting from $\mathbf{z}_0$, all $\mathbf{z}_k$ can be computed recursively, and the corresponding $\mathbf{y}_k$ recovered via

$$\mathbf{y}_{k+1} = HXH^T\mathbf{y}_k, \quad k = 0, 1, \ldots. \tag{5.20}$$

The transfer matrix X is obtained as follows. Substituting (5.19) into the second equation of (5.18) gives

$$(-A + \xi^{1/2}KX - \xi A^T X^2)\mathbf{z}_0 = 0.$$

Since $\mathbf{z}_0$ is arbitrary, X satisfies the quadratic matrix equation

$$\xi A^T X^2 - \xi^{1/2}KX + A = 0. \tag{5.21}$$

The k-th equation in (5.18) can be rewritten as

$$R_1\begin{pmatrix} \mathbf{z}_k \\ \mathbf{z}_{k-1} \end{pmatrix} = R_2\begin{pmatrix} \mathbf{z}_{k+1} \\ \mathbf{z}_k \end{pmatrix}, \tag{5.22}$$

where

$$R_1 = \begin{pmatrix} \xi^{1/2}K & -A \\ I & 0 \end{pmatrix}, \quad R_2 = \begin{pmatrix} \xi A^T & 0 \\ 0 & I \end{pmatrix}. \tag{5.23}$$

For $k = 1$, setting $\mathbf{z}_0 = \mathbf{g}$ (where $X\mathbf{g} = \lambda\mathbf{g}$) yields

$$R_1\begin{pmatrix} \lambda\mathbf{g} \\ \mathbf{g} \end{pmatrix} = \lambda R_2\begin{pmatrix} \lambda\mathbf{g} \\ \mathbf{g} \end{pmatrix}. \tag{5.24}$$

Thus, λ and $\begin{pmatrix} \lambda\mathbf{g} \\ \mathbf{g} \end{pmatrix}$ are a generalized eigenvalue and eigenvector of the pencil $R_1 - \lambda R_2$. Solving this generalized eigenvalue problem provides $2n$ eigenvalues and eigenvectors, where n is the dimension of $\mathbf{z}_k$. We select the n eigenvalues with $|\lambda| < 1$, corresponding to solutions that decay at infinity, along with their associated eigenvectors, to construct X.

The transfer matrix is given by

$$X = T\Lambda T^{-1}, \tag{5.25}$$

where Λ is the diagonal matrix of the selected eigenvalues, and T is the matrix whose columns are the corresponding $\mathbf{g}$ vectors extracted from the lower halves of the generalized eigenvectors.

This procedure, known as the infinite element method, is detailed in [27, 28] (pp. 120–126). The algorithm presented here applies to the homogeneous case $\widetilde{\mathbf{f}} = 0$. For the inhomogeneous case $\widetilde{\mathbf{f}} \neq 0$, the method extends by incorporating load vectors in each layer during assembly, with the transfer matrix handling the propagation of solutions outward.

6. Numerical Experiments

We consider the exterior domain Ξ, the meridional section of a cylinder with radius 1 and generator length 2, taking half the section due to symmetry. The triangulation $\mathcal{T}_h$ in layers Ξ_1 and Ξ_2 for $N = 33$ nodes is shown in Figure 2. Experiments vary N (number of nodes on each Γ_k) and the similarity parameter ξ.

Example 1. We solve the Stokes problem from [11] with exact solution

$$\widetilde{\mathbf{u}} = \left(-\frac{3rz}{16(r^2+z^2)^{5/2}}, \frac{r^2-2z^2}{16(r^2+z^2)^{5/2}} \right), \quad \widetilde{p} = 0, \quad \widetilde{\mathbf{f}} = 0,$$

and boundary values $\widetilde{\mathbf{g}}_1, \widetilde{\mathbf{g}}_2$ derived from the exact solution. Figures 3–4 show computed and exact components u_h and v_h on Γ_{20} for $\xi = 1.20$ ($N = 65$) and $\xi = 1.30$ ($N = 17$), respectively. The results indicate better accuracy for u_h than v_h due to singularities on the z-axis, with errors increasing with ξ. Table 1 shows first-order convergence in the $\mathbf{L}^2_1$ norm, consistent with [11]. Table 2 lists errors for $N = 65$ across different ξ, showing reduced errors as ξ decreases.

Table 1. Convergence order in domain $(r, z) \in \bigcup_{k=1}^{20} \Xi_k$

N	ξ	$\|\widetilde{\mathbf{u}} - \widetilde{\mathbf{u}}_h\|_{\mathbf{L}^2_1} \times 10^4$	order
17	1.40	5.12920	
33	1.30	1.92890	1.4114
65	1.20	0.57379	1.7225
129	1.15	0.23240	1.2987

Table 2. Errors with $N = 65$ in domain $(r, z) \in \bigcup_{k=1}^{20} \Xi_k$

ξ	$\|\widetilde{\mathbf{u}} - \widetilde{\mathbf{u}}_h\|_{\mathbf{L}^2_1} \times 10^3$
2.40	2.22901
2.10	1.73340
1.80	1.09820
1.50	0.45893
1.20	0.05737
1.15	0.02973

Example 2. We solve the Brinkman problem (3.1)–(3.4) with $\widetilde{p} = 0$, $\widetilde{\mathbf{f}} = 0$, and the same boundary values as in Example 1. Due to the absence of an analytical solution, we compare computed solutions across mesh refinements. Figures 5–7 show u_h and v_h on Γ_{20} for $N = 65$, $\xi = 1.20$, and $\varkappa = 1, 10, 25$, respectively. The results exhibit similar convergence behavior to the Stokes case, with $\varkappa$ having minimal impact on stability. Table 3 reports the norms $\|\widetilde{\mathbf{u}}_h - \widetilde{\mathbf{u}}_{h/2}\|_{\mathbf{L}^2_1}$ and $\|\widetilde{\mathbf{u}}_{h/2} - \widetilde{\mathbf{u}}_{h/4}\|_{\mathbf{L}^2_1}$ for varying $\varkappa$, confirming first-order convergence. This validates the robustness of the infinite element method for the Brinkman problem across a range of permeability parameters.

Table 3. Convergence order with $\xi = 1.20$ in domain $(r, z) \in \bigcup_{k=1}^{20} \Xi_k$

$\varkappa$	$\|\widetilde{\mathbf{u}}_h - \widetilde{\mathbf{u}}_{h/2}\|_{\mathbf{L}_1^2} \times 10^5$	$\|\widetilde{\mathbf{u}}_{h/2} - \widetilde{\mathbf{u}}_{h/4}\|_{\mathbf{L}_1^2} \times 10^5$	order
0.0	0.20778	0.03037	2.77
1.0	0.22669	0.04252	2.14
10.0	0.55954	0.15866	1.81
25.0	0.85958	0.31020	1.47
50.0	1.3370	0.61196	1.12
100.0	2.6281	1.4110	0.89

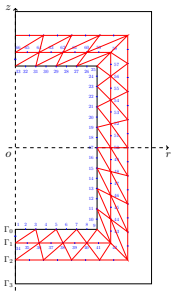

Figure 2. Triangulation with $N = 33$ in the first and second layers.

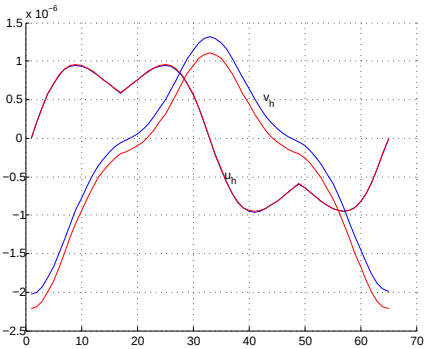

Figure 3. Computed and exact u_h and v_h on Γ_{20} with $N = 65$, $\xi = 1.2$, $\varvarkappa = 0$ (Stokes case).

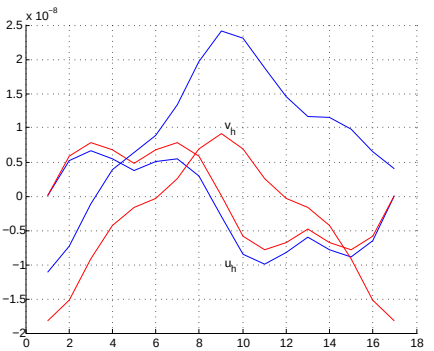

Figure 4. Computed and exact u_h and v_h on Γ_{20} with $N = 17$, $\xi = 1.3$, $\varkappa = 0$ (Stokes case).

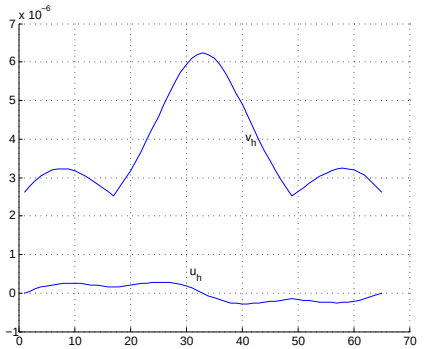

Figure 5. Computed u_h and v_h on Γ_{20} with $N = 65$, $\xi = 1.2$, $\varkappa = 1$ (Brinkman case, no exact solution available).

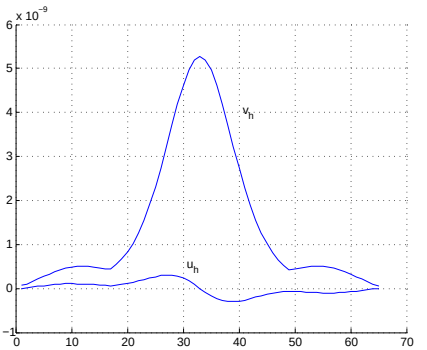

Figure 6. Computed u_h and v_h on Γ_{20} with $N = 65$, $\xi = 1.2$, $\varkappa = 10$ (Brinkman case, no exact solution available).

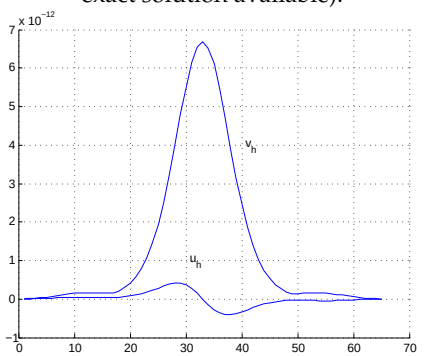

Figure 7. Computed u_h and v_h on Γ_{20} with $N = 65$, $\xi = 1.2$, $\varkappa = 25$ (Brinkman case, no exact solution available).

7. Conclusion

This study introduces a novel application of the infinite element method, inspired by Ying [27, 28], for the numerical approximation of the axisymmetric Brinkman flow in three-dimensional exterior domains. By extending the foundational work of Fang and Liao [11] on the axisymmetric Stokes problem, we have developed a robust computational framework that effectively handles the challenges posed by the Brinkman equations, particularly in unbounded domains. Our approach offers a compelling alternative to traditional boundary element methods [6, 22, 17], which are commonly employed for exterior problems but can be computationally intensive.

The numerical experiments conducted for both the Stokes and Brinkman problems demonstrate the method's stability and first-order convergence under the $\mathbf{L}_1^2$ norm across a wide range of inverse permeability parameters $\varkappa$. Notably, the infinite element method remains effective even for coarse meshes and large values of $\varkappa$, confirming its robustness in scenarios where the PDE coefficients exhibit high variability. The ability to maintain accuracy in large unbounded domains further underscores the method's versatility, making it suitable for practical applications in fields such as underground water hydrology, petroleum engineering, and biomedical engineering, where the Brinkman model is prevalent.

A key merit of this work lies in its comprehensive validation of the infinite element method for the Brinkman problem, building on the well-posedness established for the axisymmetric Stokes system [4, 12, 13, 5, 3]. The method's implementation, detailed in Section 5, leverages a transfer matrix approach to efficiently handle the infinite domain, offering computational advantages over methods requiring domain truncation. The numerical results, presented in Section 6, confirm that the method achieves consistent convergence behavior, with errors decreasing as the mesh is refined and the similarity parameter ξ is adjusted, aligning with theoretical expectations [11].

In summary, this work advances the numerical treatment of axisymmetric Brinkman flow by demonstrating the efficacy of the infinite element method in exterior domains. Future research will explore the method's performance in non-homogeneous cases ($\widetilde{\mathbf{f}} \neq 0$) and investigate its applicability to more complex geometries and coupled flow problems. These extensions will further enhance the method's utility in addressing real-world fluid dynamics challenges.

References

[1] Allaire, G. Homogenisation of the Navier-Stokes equations in open sets perforated with tiny holes II: Non-critical sizes of the holes for a volume distribution and a surface distribution of holes. *Arch. Ration. Mech. Anal.* **113** (1991), 261–298.

[2] Anaya, V.; Mora, D.; Ruiz-Baier, R. Pure vorticity formulation and Galerkin discretisation for the Brinkman equations. *IMA J. Numer. Anal.* **37** (2017), no. 4, 2020–2041.

[3] Belhachmi, Z.; Bernardi, C.; Deparis, S. Weighted clement operator and application to the finite element discretization of the axisymmetric Stokes problem. *Numer. Math.* **105** (2006), no. 2, 217–247.

[4] Bernardi, C.; Raugel, G. Analysis of some mixed finite element methods for the Stokes problem. *Math. Comput.* **44** (1985), no. 169, 71–79.

[5] Bernardi, C.; Dauge, M.; Maday, Y. *Spectral methods for axisymmetric domains*. Gauthier-Villars, Editions Scientifiques et Médicales, Elsevier, Paris, 1999.

[6] Boeckle, C.; Wittwer, P. Artificial boundary conditions for stationary Navier–Stokes flows past bodies in the half-plane. *Computers & Fluids.* **82** (2013), no. 15, 95–109.

[7] Burman, E.; Hansbo, P. Stabilized Crouzeix-Raviart element for the Darcy-Stokes problem. *Numerical Methods for Partial Differential Equations.* **21** (2005), 986–997.

[8] Burman, E.; Hansbo, P. A unified stabilized method for Stokes' and Darcy's equations. *Journal of Computational and Applied Mathematics.* **198** (2007), 35–51.

[9] Correa, M. R.; Loula, A.F.D. A unified mixed formulation naturally coupling Stokes and Darcy flows. *Computer Methods in Applied Mechanics and Engineering.* **198** (2009), 2710–2722.
[10] Ern, A.; Guermond, J.-L. *Theory and practice of finite elements*. Springer-Verlag New York, 2004.
[11] Fang, N.; Liao, C. Axisymmetric Stokes exterior problem and its numerical computation. *Acta Math. Appl. Sin. Engl. Ser.* **27** (2011), no. 1, 115–128.
[12] Girault, V.; Sequeira, A. A well-posed problem for the exterior Stokes equations in two and three dimensions. *Arch. Ration. Mech. Anal.* **114** (1991), 313–333.
[13] Girault, V.; Raviart, P.-A. *Finite element methods for navier-stokes equations: theory and algorithms*. Springer-Verlag, Berlin, 1986.
[14] Gutt, R.; Kohr, M., Mikhailov, S.E., Wendland, W. *On the mixed problem for the semilinear Darcy-Forchheimer-Brinkman PDE system in Besov spaces on creased Lipschitz domains*. Mathematical Methods in the Applied Sciences, 2017.
[15] Guzmán, J.; Neilan, M. *A family of nonconforming elements for the Brinkman problem*. IMA Journal of Numerical Analysis, 2012.
[16] Hannukainen, A.; Juntunen, M., Stenberg, R. Computations with some finite element methods for the Brinkman problem. *Computational Geosciences.* **15** (2011), 155–166.
[17] Heltai, L.; Arroyo, M., DeSimone, A. Nonsingular isogeometric boundary element method for Stokes flows in 3D. *Computer Methods in Applied Mechanics and Engineering*. **268** (2014), no. 1, 514–539.
[18] Kohr, M.; Wendland, W.L. Boundary integral equations for a three-dimensional Brinkman flow problem. *Math. Nachr.* **282** (2009), no 9, 1305–1333.
[19] Kohr, M.; Mikhailov, S.E.; Wendland, W.L. Transmission Problems for the Navier-Stokes and Darcy-Forchheimer-Brinkman Systems in Lipschitz Domains. *Journal of Mathematical Fluid Mechanics.* **19** (2016), no. 2.
[20] Kohr, M.; Medkova, D.; Wendland, W.L. On the Oseen-Brinkman flow around an (m-1) dimensional solid obstacle. *Monatshefte fur Mathematik.* **183** (2017), no. 2, 269–302
[21] Könnö, J.; Stenberg, R. Numerical computations with $H(div)$-elements for the Brinkman problem. *Computational Geoscienes.* **16** (2012), 139–158.
[22] Peng, H.F.; Cui, M.; Gao, X.W. A boundary element method without internal cells for solving viscous flow problems. *Engineering Analysis with Boundary Elements.* **37** (2013), no. 2, 293–300.
[23] Stenberg, R.; Videman, J. On the error analysis of stabilized finite element methods for the Stokes problem. *SIAM Journal of Numerical Analysis.* **53** (2015), no. 6, 2626–2633.
[24] Vassilevski, P.; Villa, U. A Mixed Formulation for the Brinkman Problem. *SIAM J. Numer. Anal.* **52** (2014), no. 1, 258–281.
[25] Xie, X.P.; Xu, J.C.; Xue, G.R. *Uniformly-stable finite element methods for Darcy-Brinkman models*. J. Comput. Math., 2008.
[26] Xiong, Y.; Chen, Y. A priori and a posteriori error estimates of a really pressure-robust virtual element method for the incompressible Brinkman problem. *arXiv:2411.16067v2 [math.NA]*, 2024.
[27] Ying, L. *Infinite element methods*. Peking University Press. Beijing and Vieweg and Sohn Verlagsgesellschaft, mbH, Braunschweig/wiesbaden, 1995.
[28] Ying, L. *Numerical Methods for Exterior problems*. World Scientific, Singapore, 2006.

[1] Laboratory of SD, Faculty of mathematics University of Science and Technology Houari Boumediene (USTHB), 16111 Algiers, Algeria
Email address: KMhamedMessaoud@gmail.com

[2] Laboratory of SD, Faculty of mathematics University of Science and Technology Houari Boumediene (USTHB), 16111 Algiers, Algeria
Email address: rabahhacenebellout@gmail.com

[3] Laboratory of SD, Faculty of mathematics University of Science and Technology Houari Boumediene (USTHB), 16111 Algiers, Algeria
Email address: toufik.laadj@usthb.edu.dz